

with target nucleons, the null value of the analyzing power indicates that formation of complex fragments does not proceed via a simple direct reaction mechanism.

1. S.J. Yennello, *et al.*, Phys. Rev. C **42**, 79 (1990).
2. R.E.L. Green, *et al.*, Phys. Rev. C **22**, 1594 (1980).
3. R.E.L. Green, *et al.*, Phys. Rev. C **25**, 828 (1982).

IMF EMISSION IN THE $^{14}\text{N} + {}^{nat}\text{Ag}, \text{Au}$ REACTIONS
AT $E/A = 60\text{-}100$ MeV

J.L. Wile, D.E. Fields, K. Kwiatkowski, K.B. Morley, E. Renshaw,
V.E. Viola, and S.J. Yennello
Indiana University Cyclotron Facility, Bloomington, Indiana 47405

R.T. de Souza, C.K. Gelbke, W.G. Lynch, M.B. Tsang, W.G. Gong,
H.M. Xu, and N. Carlin
*National Superconducting Cyclotron Laboratory, Michigan State University,
East Lansing, Michigan 48824*

In a recent study^{1,2} of IMF emission in the $^{14}\text{N} + {}^{nat}\text{Ag}, \text{Au}$ systems at bombarding energies of 20 to 50 MeV per nucleon, three sources of intermediate mass fragment (IMF) production were reported. The most important emission source at low bombarding energies produced IMFs with kinetic energies near the Coulomb repulsion energy and angular distributions that were relatively isotropic. The energy and angular distributions of these IMFs were well described by the model of Moretto;³ thus, this source was identified with emission from a fully equilibrated compound nucleus. In addition to this "equilibrium" source, two other sources were observed. The first of these was associated with projectile fragmentation-like events and was analyzed using the empirical model of Kiss, *et al.*⁴ The remaining source of IMF production grew in importance as the bombarding energy was increased. The IMFs produced by this "non-equilibrium" source are highly energetic and strongly forward-focused, and they constitute a significant part of the total cross section well-beyond the grazing angle. These characteristics tend to indicate that the emission takes place on a relatively short time scale. However, polarization studies⁵ imply that these IMFs retain no memory of the initial beam polarization, therefore, the projectile must undergo several collisions with target nucleons before the IMF emission takes place.

In order to shed more light on the underlying mechanisms of IMF emission, as well as to investigate the possible emergence of multifragmentation as a source for IMF production, the systematics of the previous $^{14}\text{N} + {}^{nat}\text{Ag}, \text{Au}$ studies were extended to 100 MeV per nucleon. The experiment took place at the MSUNSCL K1200 cyclotron, which delivered ^{14}N beams of 60, 80, and 100 MeV per nucleon. High-purity, self-supporting targets of ^{nat}Ag and ^{nat}Au were surrounded by seven IMF detector telescopes at 20, 50, 70, 90, 120, 140, and 160 degrees in the laboratory. The detector telescopes consisted of a CF_4

gas-ionization chamber followed by a combination of silicon strip detectors, lithium-drifted silicon detectors, and cesium-iodide crystals viewed by silicon PIN diodes. The 20 degree detector was positioned on a moveable arm and also sampled data at 35 degrees in the laboratory. Inclusive data were recorded for both targets, and the carbon contamination of the targets was found to be negligible by comparison of the silver and gold data to short runs with a carbon target.

An example of the energy spectra of boron fragments from the reaction $^{14}\text{N} + ^{\text{nat}}\text{Ag}$ at $E_{\text{lab}} = 80$ MeV per nucleon is shown for all detection angles in Fig. 1. Examination of the figure reveals the same IMF characteristics as reported previously, i.e., high kinetic energy fragments whose cross sections drop sharply as the laboratory angle increases, and low kinetic energy fragments at backward angles whose angular distributions are rather isotropic. The data were separated into equilibrium (dotted curve), non-equilibrium (dashed curve), and projectile fragmentation (dot-dashed curve) sources by utilizing a simultaneous, three-source fitting procedure.² The total fit (solid curve) does an excellent job of describing the energy spectra at all angles. One interesting result from this fit is that at 100 MeV per nucleon, the temperature parameter of the equilibrium source, averaged over all elements

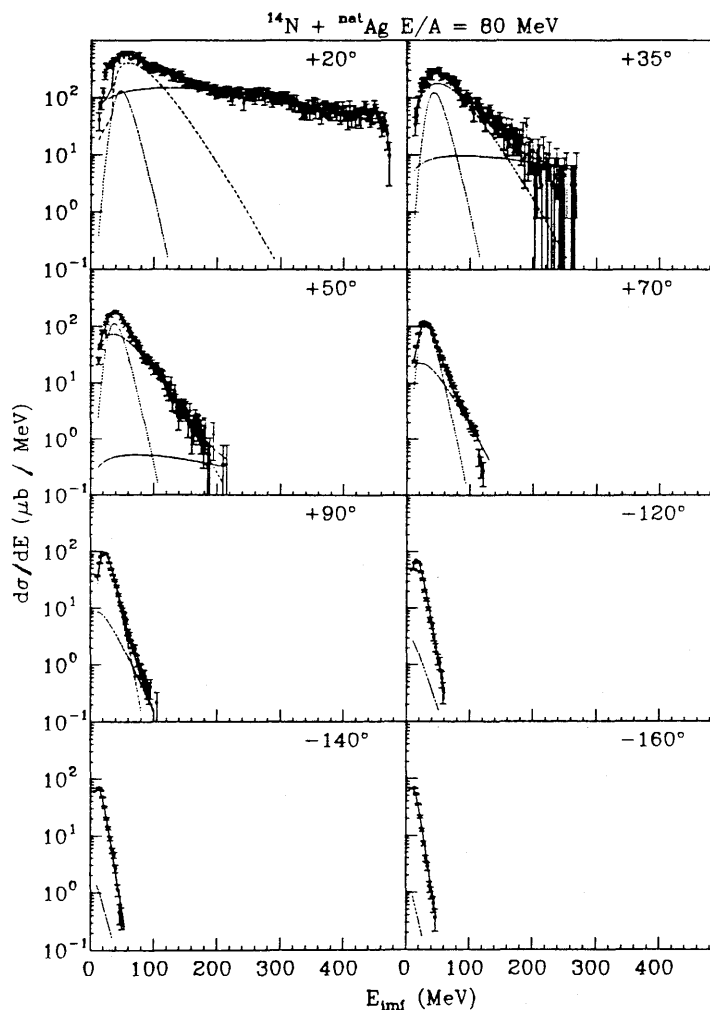
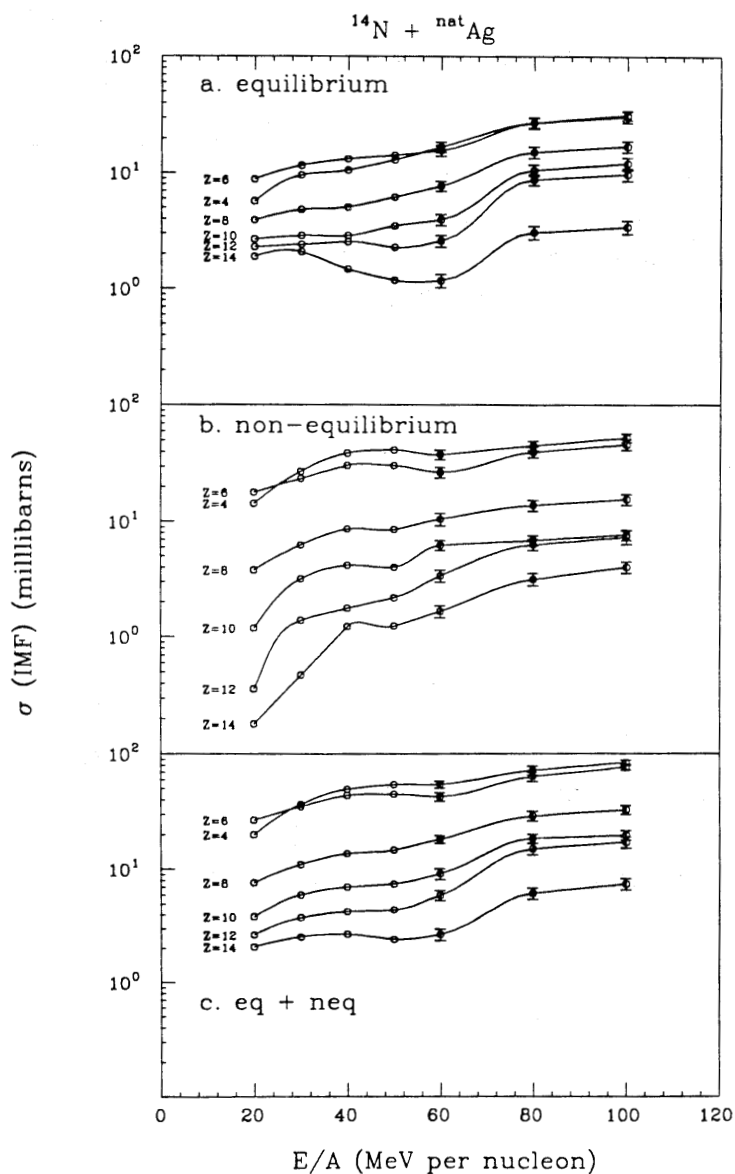


Figure 1. Energy distributions of boron fragments from the reaction $^{14}\text{N} + ^{\text{nat}}\text{Ag}$, at $E/A = 80$ MeV. The solid curves illustrate the results of a simultaneous fit which assumes IMF emission from equilibrium (dotted), non-equilibrium (dashed), and projectile fragmentation (dot-dashed) sources. The angles indicated are in the laboratory.

detected, was $(7.1 \pm 0.8 \text{ MeV})$. If this parameter is interpreted as the actual temperature of the compound nucleus, then the data indicate that nuclei can thermalize significantly more excitation energy than predicted,⁶ at least for this subset of the reaction cross section.

The fit discussed above allows an identification of the three IMF sources, and a determination of the IMF production cross sections from each of these sources. Fig. 2 illustrates the behavior of the equilibrium (Fig. 2a) and non-equilibrium (Fig. 2b) emission cross sections for even-Z elements as a function of bombarding energy over the entire range spanned

Figure 2. IMF production cross sections for even-Z fragments from equilibrium (a), non-equilibrium (b), and both (c) sources as a function of bombarding energy. Only even-Z elements are represented. The solid curves are meant to guide the eye.

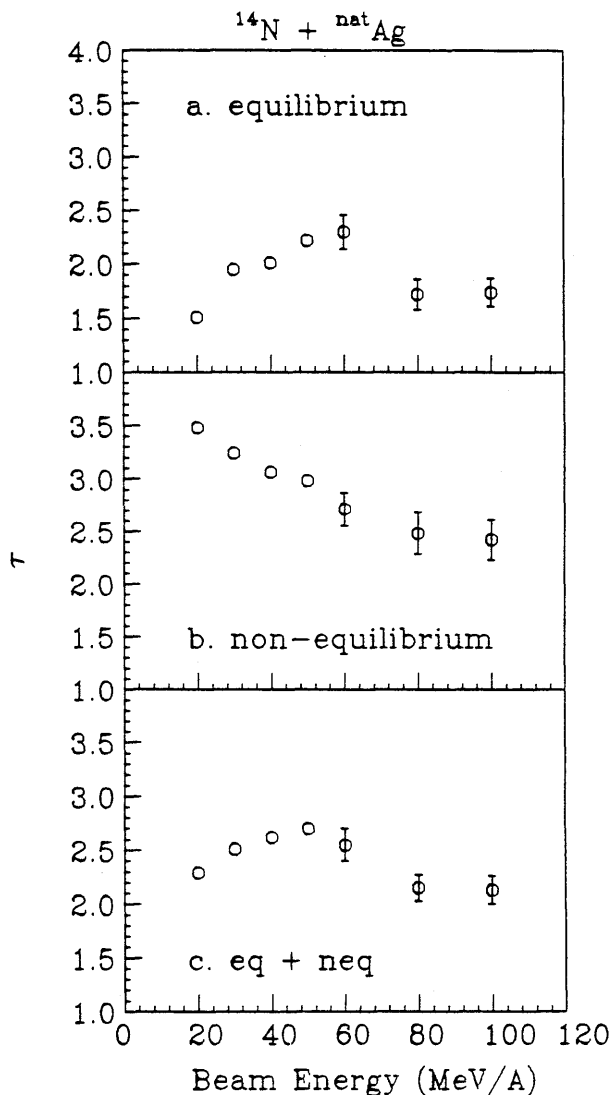


by both this experiment and the one of Ref. 2. Although the data indicate that the evolution of the IMF production cross sections is rather smooth over the energy range studied, a few points are noted. First, the equilibrium emission cross sections tend to increase more rapidly for the heavier elements ($Z \geq 10$) than for the lighter ones between

60 and 80 MeV per nucleon. In the 80 to 100 MeV per nucleon range, however, the cross sections for all elements saturate. Second, while this trend is quite clear for the equilibrium source, the cross sections for IMFs produced by the non-equilibrium source do not behave in a similar manner. For all elements, the non-equilibrium IMF production cross sections seem to saturate over the 60 to 100 MeV per nucleon range. The total summed cross sections (Fig. 2c) exhibit trends that essentially mirror those of the equilibrium cross sections.

The emission cross sections for all elements were fit as a function of atomic number with a simple power law parameterization, $(\sigma(Z) \propto Z^{-\tau})$ and the results of this fit are shown in Fig. 3. The figure shows that for the equilibrium (Fig. 3a) and summed (Fig. 3c) IMF production sources, the character of the Z distributions, as illustrated by the τ parameters, changes abruptly over the 60 to 80 MeV per nucleon range. The change in the τ parameters is actually the result of the contribution of the heavier elements as illustrated in Fig. 2. Once again, while this change is quite apparent for the two sources mentioned above, the τ parameters characterizing the Z distributions of IMFs from the non-equilibrium source do not exhibit this abrupt change in slope.

Figure 3. The results of a fit of the IMF charge distributions using a simple $Z^{-\tau}$ parameterization for (a) the equilibrium, (b) non-equilibrium, and (c) the sum of the two, and sources.



The inclusive nature of this experiment precludes any clear statement concerning both the nature of and reason for this abrupt change in emission source topology. One possible explanation would be that angular momentum is playing a more important role at higher energies, thus increasing the importance of heavy element emission from the equilibrated compound nucleus. Another possibility would be that sequential or instantaneous multifragmentation, which should be characterized by a significantly different charge distribution, may be enhancing the yield of heavy elements in the equilibrium emission source beyond $E/A \approx 50$ MeV. Clearly, further investigations of an exclusive nature utilizing detector systems with a large geometric efficiency must be performed to examine this phenomenon more closely.

1. D.E. Fields, *et al.*, MSU Cyclotron Laboratory Annual Report, 1987, p.27.
2. D.E. Fields, *et al.*, Phys. Lett. **B220**, 356 (1989).
3. L.G. Moretto, *et al.*, Nucl. Phys. **A247**, 211 (1975).
4. A. Kiss, *et al.*, Nucl. Phys. **A499**, 131 (1989).
5. E. Renshaw, private communication.
6. D.H.E. Gross, Nucl. Phys. **A437**, 643 (1985).

OCTUPOLE CORRELATIONS IN $^{145,146}\text{Nd}$ NUCLEI

W. Urban, J.C. Bacelar, O. Dermois and J. Jongman
Kernfysisch Versneller Instituut, Groningen, The Netherlands

P.P. Singh
Indiana University, Bloomington, Indiana 47405

For the ^{146}Nd nucleus, calculations indicate an enhancement of octupole correlations at medium spins.¹ It has been predicted that with increasing rotational frequency a reflection-asymmetric structure should become yrast. In this work we aimed to verify this prediction. To populate high spins in ^{146}Nd , we utilized the $^{136}\text{Xe}+^{13}\text{C}$ compound nucleus reaction using a solidified ^{136}Xe target and 54 MeV ^{13}C beam from the KVI cyclotron. The $\gamma - \gamma$ coincidences were collected with 4 Ge detectors in anti-Compton shields. The level scheme resulting from these data is shown in Fig. 1a. An interesting result of the present work is an extension of the ground state, alternating-parity band up to spin $I=14$. It is possible, though at present still speculative that the $I=18$ level at 5900.5 keV and the $I=19$, level at 6195.0 keV are also members of this band. An analogous 18 and 19 levels have been found at similar excitation energies in other $N=86$ nuclei.

The above observations support the prediction that the octupole correlations extend in ^{146}Nd to high spins. As in ^{148}Sm one observes here a competition between octupole and single-particle, reflection-symmetric excitations. The presence of a short cascade built on top of the 8^+ , 2475.1 keV level and the $(f_{7/2}^2)_{2+,4+,6+}$ excitations on top of the